

Theoretical Studies on the Competitive S_N2 Reactions of O-Imidomethyl Derivatives of Phenols with OH⁻

Chang Kon Kim, Dong Soo Chung, Chan Kyung Kim, Bon-Su Lee,^{*}
Yeong-Jin Chung,[†] Byung Choon Lee,[‡] and Ikchoon Lee

Department of Chemistry, Inha University, Incheon 402-751, Korea

[†]Chemistry Division, Samchok National University, Samchok 245-711, Korea

[‡]Department of Chemistry, Choongbuk National University, Chongju 361-763, Korea

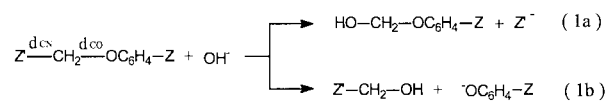
Received September 1, 2000

Nucleophilic substitution reactions of O-imidomethyl derivatives of phenols with OH⁻ were studied theoretically using the semiempirical AM1 and Solvation Model 2.1 (SM2.1) methods in the gas phase and aqueous solution, respectively. In the gas phase, the two reaction paths, in which the imide (1a) or phenol (1b) is functioning as a leaving group, can occur competitively. In contrast, in aqueous solution, path (1b) becomes more favorable than (1a) because the transition states (TS) of path (1b) are more stabilized by solvent. Differences in solvation energies are caused by the structural differences of TS, *i.e.*, the TS *via* path (1b) is more dissociative than that *via* path (1a). Therefore we conclude that the solvent effects play an important role in the hydrolysis of O-imidomethyl derivatives of phenols. However, reactivity is dependent on the acidities of both the imide and the phenol fragments since the ρ_z values vary progressively from 4.2 (Z' = I) to 2.5 (Z' = IV) as the acidities of imide increase. These are in good agreement with the experimental results.

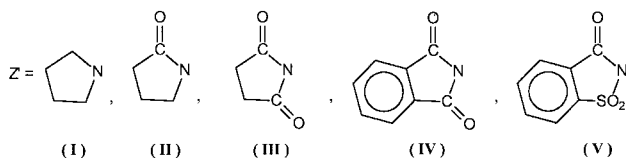
Keywords: Competitive S_N2, AM1-SM2.1, O-Imidomethyl Derivatives, TS-Solvation.

Introduction

Recently, Getz *et al.* have reported the studies on the reaction mechanism of hydrolysis of O-imidomethyl derivatives of phenols.¹ This reaction is important because O-imidomethyl derivatives of phenols can serve as prodrugs of phenolic drugs.² The hydrolysis of O-imidomethyl derivatives in basic solution (pH > 7.0) is a typical substitution reaction without the possibility of elimination, since no hydrogen atom is attached to the β -position of the leaving group. However, the substitutions can be competitive because two pathways are possible as represented in Eqs. (1), *i.e.*, imide or phenol portion can competitively acts as a leaving group.



Z = H, p-F, p-Cl, p-CN, p-NO₂



The proposed mechanism by Getz *et al.*¹ for the hydrolysis was an S_N2 reaction of Eq. (1b) where the phenol group functioned exclusively as a nucleofuge. Even in the case of

the best leaving group as saccharin (V), the reaction mechanism did not change. However the rates of the hydrolysis were dependent on the acidities of both the imide and the phenol fragments though they were more sensitive to the acidity of the phenol.

Nevertheless some questions are still remained unanswered for the proposed mechanism, since the reactants used were limited to a very strong electron-withdrawing phenol (Z=NO₂). Therefore, in order to elucidate the hydrolysis mechanism of O-imidomethyl derivatives more thoroughly, we have studied theoretically the S_N2 reactions by varying the imido group as well as phenol substituent in the gas phase and in solution.

Calculation

For the gas phase reactions, the semi-empirical AM1 method³ in MOPAC 6.0 package⁴ was employed to conserve computational time, since the reaction systems considered in this study are relatively large and the use an *ab initio* method is out of question. All stable structures, reactants (R) and products (P), were fully optimized using the energy gradient method. Transition states (TS) were located using the non-linear least square (NLLSQ) or TS options starting from the highest energy point determined previously using the reaction coordinate method.⁵ Frequency calculations were also performed to confirm all positive frequencies for the stable structures and one negative imaginary frequency for the TS.⁶ Substituents (Z) of phenol moiety used in the calculation have strong electron withdrawing property because even the electron donating substituent acts as a electron acceptor in the anionic reaction system, which made direct

^{*}Corresponding Author. Fax: +82-32-873-9333, e-mail: bslee@inha.ac.kr

comparison with experiment difficult.

To obtain the solvation Gibbs free energy (ΔG_s) in aqueous solution, the SM2.1 method⁷ implemented in AMSOL 5.0 package⁸ was used. In the SM2.1 calculations, solvation energy was obtained using the gas-phase optimized geometry (SM2.1//AM1) due to problems associated with the convergence and computational time. The Gibbs free energy changes (ΔG_{aq}) in aqueous solution were then obtained using Eq. (2), where ΔG_g^\ddagger refers to the gas-phase free energy change and $\delta\Delta G_{\text{sol}}$ to the solvation free energy change.

$$\Delta G_{\text{aq}} = \Delta G_g + \delta\Delta G_s \quad (2)$$

Results and Discussion

As shown in Eqs. (1), the two reaction paths can occur competitively. Therefore we assume that the relative reactivities will depend upon the leaving ability of a nucleofuge. In order to compare the nucleofugicities of the leaving groups, the proton affinities (PA) of Z'^- and ${}^-\text{OC}_6\text{H}_4\text{Z}$ were calculated and the results are collected in Table 1. As shown in Table 1, the PAs of I and II were much larger (> 20 kcal mol⁻¹) than those of phenolate anions. However the PAs of III-V are comparable to, or smaller than, those of phenolate anions, e.g., the PAs of III and ${}^-\text{OC}_6\text{H}_5$ are nearly the same and the PA of V is very similar to that of $\text{OC}_6\text{H}_4\text{CN}^-$. This suggests that the reaction mechanism can change depending on the relative PAs of the leaving groups.

The calculated enthalpy (ΔH^\ddagger), entropy ($-T\Delta S^\ddagger$) and Gibbs free energy change (ΔG_g^\ddagger) of activation as well as heat of formation (ΔH_f°) of R with Z=H in the gas phase are summarized in Table 2. As expected from the PAs discussed above, the ΔH^\ddagger and/or ΔG_g^\ddagger of reaction path (1b), in which phenolate is the leaving group, is more favorable than that of reaction path (1a), in which the imide is a leaving group, for $Z' = \text{I}$ and **II**. The ΔG_g^\ddagger for paths (1a) and (1b) are reversed for $Z' = \text{III}$, **IV** and **V**. Moreover the ΔG for $Z' = \text{V}$ of path (1a) is still more favorable by 0.3 kcal mol⁻¹ than that of path (1b) with the best leaving group $Z = \text{NO}_2$ (data not shown).

Table 1. Calculated proton affinities (PA)^a of imide and phenol in kcal mol⁻¹

A ⁻ + H ⁺ ⇌ AH	
A	PA
I	-394.21
II	-362.31
III	-346.85
IV	-343.75
V	-332.28
OC_6H_5	-346.97
$\text{OC}_6\text{H}_3\text{F}$	-341.12
$\text{OC}_6\text{H}_3\text{Cl}$	-339.70
$\text{OC}_6\text{H}_3\text{CN}$	-331.22
$\text{OC}_6\text{H}_3\text{NO}_2$	-320.26

^aPA = $\Delta H_f^\circ(\text{AH}) - [\Delta H_f^\circ(\text{A}^-) + \Delta H_f^\circ(\text{H}^+)]$ where $\Delta H_f^\circ(\text{H}^+) = 367.2$ kcal mol⁻¹ was used. Dewar, M. J. S.; Dieter, K. M. *J. Am. Chem. Soc.* **1986**, *108*, 8075.

Table 2. Calculated heats of formation (ΔH_f°) of reactant and enthalpy (ΔH^\ddagger), entropy ($-T\Delta S^\ddagger$) and Gibbs free energy change (ΔG_g^\ddagger) of activation^a for the reaction systems with Z = H in the gas phase at 298 K

Z'	Path	$\Delta H_f^\circ(\text{R})$	ΔH^\ddagger	$-T\Delta S^\ddagger$	ΔG_g^\ddagger	ΔG_g^\ddagger
I	(1a)	-26.0	12.6	11.6	24.2	-28.0
	(1b)		-8.6	10.9	2.3	-70.5
II	(1a)	-60.3	-1.6	11.5	9.9	-58.6
	(1b)		-8.4	10.7	2.3	-70.2
III	(1a)	-90.2	-10.7	9.6	-1.1	-79.5
	(1b)		-8.6	8.0	-0.6	-73.3
IV	(1a)	-39.0	-11.6	9.7	-1.9	-82.5
	(1b)		-8.3	8.1	-0.2	-73.4
V	(1a)	-73.5	-17.5	10.2	-7.3	-88.9
	(1b)		-11.0	8.9	-2.1	-67.7

^aIn kcal mol⁻¹

These results are inconsistent with the experimental results in aqueous solution, i.e., Getz *et al.* have reported that the phenol group functioned as a nucleofuge even in the case of $Z' = \text{V}$. We can assume that this might be caused by the solvent effects. Thus we calculated the solvation free energy (ΔG_s) in aqueous solution using the SM2.1 method mentioned above. Calculated ΔG_s of R, TS and P and Gibbs free energy of reaction, $\Delta G_{\text{aq}}^\ddagger$, for Z = H, obtained using Eq. (2) are summarized in Table 3. Activation free energies for full reaction system, Eq. (1), are collected separately in Table 4. Examination of Table 4 shows that the activation free energy in solution, $\Delta G_{\text{aq}}^\ddagger$, is much higher than ΔG_g^\ddagger in the gas phase since the solvation free energy of reactants, $\Delta G_s(\text{R})$, is much larger than that of TSs, $\Delta G_s(\text{TS})$, due to the large solvation energy of OH⁻ (see Table 3). Calculated ΔG_s of OH⁻ agrees well with the experimental values (104-110 kcal mol⁻¹).⁹ The higher $\Delta G_{\text{aq}}^\ddagger$ compared to ΔG_g^\ddagger is consistent with the Hughes-Ingold rules,¹⁰ i.e., the activation energy rises as the negative charge density is dispersed at the TS compared to the reactants. Similarly, reaction free energy in aqueous solution, $\Delta G_{\text{aq}}^\circ$, is also much larger than ΔG_g° in the gas phase (Table 2), since negative charge densities are more

Table 3. Calculated the Gibbs free energies of solvation (ΔG_s), activation ($\Delta G_{\text{aq}}^\ddagger$) and reaction ($\Delta G_{\text{aq}}^\circ$) in aqueous solution in kcal mol⁻¹ for the reaction systems with Z = H

Z'	Path	$\Delta G_s(\text{R})^a$	$\Delta G_s(\text{TS})$	$\Delta G_s(\text{P})$	$\Delta G_{\text{aq}}^\circ$ ^b
I	(1a)	-115.6	-51.9	-61.5	26.1
	(1b)		-63.4	-70.9	-25.9
II	(1a)	-119.4	-62.2	-75.2	-14.4
	(1b)		-67.1	-75.7	-26.6
III	(1a)	-121.6	-65.1	-72.3	-30.2
	(1b)		-73.9	-77.1	-28.9
IV	(1a)	-121.2	-65.3	-71.3	-32.6
	(1b)		-74.5	-76.5	-28.7
V	(1a)	-128.2	-67.2	-70.9	-31.6
	(1b)		-70.3	-84.0	-23.5

^a $\Delta G_s(\text{OH}^-) = -110.0$ kcal mol⁻¹ is included. ^b $\Delta G_{\text{aq}}^\circ = \Delta G_g^\circ - [\Delta G_s(\text{P}) - \Delta G_s(\text{R})]$.

Table 4. Calculated ΔG_{aq}^\ddagger ^a in kcal mol⁻¹

Z'	Z		F		Cl		CN		NO ₂	
	1a	1b	1a	1b	1a	1b	1a	1b	1a	1b
I	87.5	54.5	86.7	52.4	85.8	51.7	84.6	48.2	84.3	46.7
II	67.1	54.5	65.1	51.5	65.0	50.9	64.7	48.9	63.3	47.1
III	55.4	47.0	55.6	45.8	55.4	45.2	55.1	42.8	55.5	40.5
IV	54.0	46.6	54.2	45.4	54.1	44.8	53.8	42.3	54.2	40.7
V	53.7	55.8	54.1	54.5	53.9	53.9	54.0	51.6	54.8	49.5

$$^a \Delta G_{aq}^\ddagger = \Delta G_g^\ddagger - [\Delta G_s(\text{TS}) - \Delta G_s(\text{R})].$$

delocalized in the product anions. These results suggest that the decrease in reactivity of the hydrolysis of O-imidomethyl derivatives of phenols is caused kinetically and thermodynamically in solution.

Inspection of Table 4 shows that ΔG_{aq}^\ddagger of path (1b) is lower than the ΔG_{aq}^\ddagger of path (1a) except for Z' = V with Z = H or F. The ΔG_{aq}^\ddagger of path (1b) for Z' = V becomes progressively more favorable than that of path (1a) as the substituent (Z) of phenol fragment becomes electron-withdrawing, e.g., ΔG_{aq}^\ddagger of paths (1b) and (1a) for Z = Cl are nearly the same and that of path (1b) for Z = NO₂ is more favorable by 5.3 kcal mol⁻¹. Experimental study on the reaction mechanism has only been performed for two representative cases (Z = NO₂ and Z' = IV or V), and our theoretical results are in agreement with the experimental results. Therefore we can conclude that the solvent effect plays an important role in the

hydrolysis of O-imidomethyl derivatives of phenols.

Reactivity difference between the two paths in the gas phase and in aqueous solution are caused by the solvation free energy differences at the TSs. $\Delta G_s(\text{TS})$, i.e., as can be seen in Table 3. $\Delta G_s(\text{TS})$ of path (1b) is much larger than that of path (1a). This can be easily understood by the inspection of TS structures. The TS structures of Z' = I and V with Z = H are depicted in Figure 1 and some selected bond lengths of the reactants and TS are collected in Table 5. Percentage bond order change ($\% \Delta n^\ddagger$) on going from reactant to TS is defined in Eq. (3)¹¹ using the Pauling's bond order definition,¹² where d_R , d^\ddagger and d_P denote the bond lengths of reactant, TS and product, respectively, and α is an arbitrary constant where we adopted $\alpha = 0.6$.^{11(b)-(c)}

$$\% \Delta n^\ddagger = \frac{\exp(-d^\ddagger/\alpha) - \exp(-d_R/\alpha)}{\exp(-d_P/\alpha) - \exp(-d_R/\alpha)} \times 100 \quad (3)$$

As can be seen in Figure 1 and Table 5, the bond length d_{CNu}^\ddagger at the TS is much longer for path (1b) than path (1a). The bond length d_{CO}^\ddagger of path (1b) is also longer than the bond length d_{CN}^\ddagger of path (1a) except for Z' = I. These bond length changes are in line with the $\% \Delta n^\ddagger$, i.e., the longer the d_{CNu}^\ddagger , the smaller is the $\% \Delta n^\ddagger$, and the longer the d_{CO}^\ddagger or d_{CN}^\ddagger , the larger is the $\% \Delta n^\ddagger$. Smaller $\% \Delta n^\ddagger$ in d_{CNu}^\ddagger indicates lesser degree of bond formation whereas smaller $\% \Delta n^\ddagger$ in d_{CO}^\ddagger or d_{CN}^\ddagger implies smaller degree of bond break-

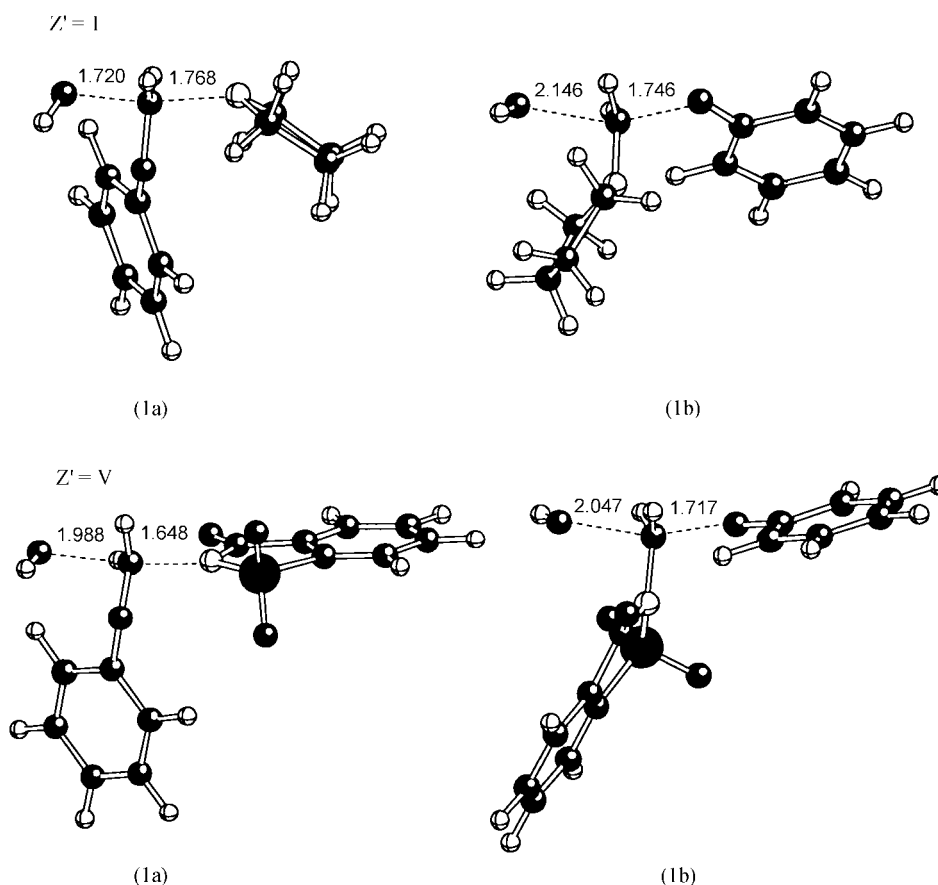
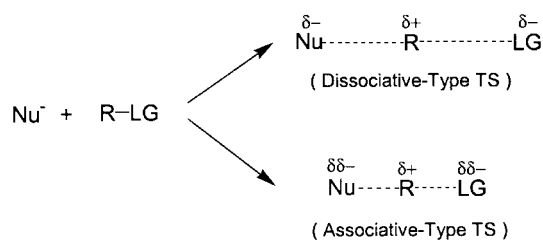
**Figure 1.** Optimized TS structures of Z' = I and V with Z = H for path (1a) and (1b) in the gas phase.

Table 5. Some selected bond lengths (d in Å) of reactants, TS and products and percentage bond order changes (% Δn^{\ddagger}) at TS for Z = H

	Path		Reactants	TS	Products	% Δn^{\ddagger}
I	(1a)	d _{CN}	1.438	1.768	–	43
		d _{CNu}	–	1.720	1.400	59
	(1b)	d _{CO}	1.445	1.746	–	39
		d _{CNu}	–	2.146	1.425	30
II	(1a)	d _{CN}	1.429	1.691	–	35
		d _{CNu}	–	1.846	1.400	48
	(1b)	d _{CO}	1.434	1.760	–	42
		d _{CNu}	–	2.130	1.420	31
III	(1a)	d _{CN}	1.438	1.661	–	31
		d _{CNu}	–	1.932	1.400	41
	(1b)	d _{CO}	1.427	1.730	–	39
		d _{CNu}	–	2.108	1.412	31
IV	(1a)	d _{CN}	1.435	1.652	–	30
		d _{CNu}	–	1.939	1.400	41
	(1b)	d _{CO}	1.428	1.723	–	39
		d _{CNu}	–	2.107	1.413	31
V	(1a)	d _{CN}	1.440	1.648	–	29
		d _{CNu}	–	1.988	1.400	38
	(1b)	d _{CO}	1.425	1.717	–	39
		d _{CNu}	–	2.047	1.411	35

**Scheme 1**

ing. Reference to Table 5 shows that the % Δn^{\ddagger} values of path (1b) are smaller for $d_{\text{CNu}}^{\ddagger}$ but larger for d_{CO}^{\ddagger} compared to d_{CN}^{\ddagger} of path (1a), respectively. This implies that the TS structure for path (1b) is more dissociative (loose) than that for path (1a). Accordingly, transfer of negative charge from nucleophile to substrate is relatively smaller but charge separation within the substrate is large in the TS leading to path (1b) as represented in Scheme 1. Therefore it is conceivable that the solvation energy is much larger for dissociative-type TS, and hence the $\Delta G_s(\text{TS})$ of path (1b) are much larger than that of path (1a).

In order to test the substituent (Z) effects of phenol moiety in aqueous solution, the Hammett, Eq. (4),¹³ and the Brønsted type correlations, Eq. (5),¹⁴ for path (1b) are examined. The σ^- values¹⁵ have been used to obtain better correlation and $\text{p}K_a$ values were taken from standard textbook¹⁶ and the calculated ρ_{Z^-} and β_{Z} values are collected in Table 6. Reference to Table 6 shows that the magnitude of ρ_{Z^-} progressively decreases from 4.2 ($Z' = \text{I}$) to 3.2 ($Z' = \text{IV}$) as the acidity of the imide increases. Also β_{Z} values shows the same trend. This is consistent with the Reactivity-Selectivity

Table 6. Calculated ρ_{Z^-} and β_{Z} values^a

Z'	ρ_{Z^-}	β_{Z}
I	4.2	1.9
II	3.5	1.5
III	3.4	1.5
IV	3.2	1.4
V	3.3	1.5

^aRegression coefficients (r) are better than 0.95.

Principle (RSP).¹⁷ The reactivities in aqueous solution are progressively increased (and hence $\Delta G_{\text{aq}}^{\ddagger}$ are decreased) as the acidities of imide portions increase since the increasing acidity imply stronger electron withdrawing power. Accordingly, the larger the reactivity (the smaller the $\Delta G_{\text{aq}}^{\ddagger}$), the lesser is the selectivity (the smaller is the ρ_{Z^-} and/or β_{Z}).

$$\frac{-\Delta G_{\text{aq}}^{\ddagger}}{2.303RT} = \rho\sigma \quad (4)$$

$$\frac{-\Delta G_{\text{aq}}^{\ddagger}}{2.303RT} = -\beta \text{p}K_a \quad (5)$$

It is not possible to compare the theoretical ρ_{Z^-} and β_{Z} values with the experimental values because the substituent, Z, used in the computation is rather limited. Even with this difficulty, comparison of two results may be meaningful. Theoretical ρ_{Z^-} values for $Z' = \text{III}, \text{IV}$ and V are nearly constant, which is similar to the experimental results (experimental ρ value are +0.47, +0.50 and +0.84 for $Z' = \text{III}, \text{IV}$ and V , respectively). Theoretical ρ values are much greater than the experimental values as already reported.¹⁸ The same trend is also found for the β_{Z} values, *i.e.*, theoretical and experimental (0.206, 0.218, 0.279 for system III, IV and V respectively) values are almost constant for the Z' groups.

Summary. Although the two reaction paths can occur competitively in the gas phase, the path (1b) becomes more favorable in aqueous solution because the TS of path (1b) is more stabilized by solvent effects. The differences in solvent effects are caused by the dissociative nature of the TS leading to path (1b). Thus we conclude that the solvent effects play a very important role in the hydrolysis of *O*-imido-methyl derivatives of phenols. On the other hand, the reactivities are dependent on the acidities of both the imide and the phenol fragments, since the ρ_{Z^-} (or β_{Z}) values decrease progressively decreased from 4.2 (1.9) to 3.2 (1.4) as the acidities of imide portions increase. These theoretical results are in good agreement with the experimental results in aqueous solution.

Acknowledgment. We thank Inha University for support of this work.

References

- Getz, J. J.; Pranker, R. J.; Sloan, K. B. *J. Org. Chem.* **1993**, *58*, 4913.
- (a) Sloan, K. B.; Koch, S. A. *J. Org. Chem.* **1983**, *48*, 3777. (b) Bodor, N.; Sloan, K. B.; Kaminski, J. J.; Shih, C.; Pogany, S. *J. Org. Chem.* **1983**, *48*, 5280.

3. Dewar, M. J. S.; Zoebisch, E. G.; Healy, E. P.; Stewart, J. J. P. *J. Am. Chem. Soc.* **1985**, *107*, 3902.
 4. MOPAC 6.0 Program, available from Quantum Chemistry Program Exchange (QCPE) No. 506.
 5. (a) Muller, K. *Angew. Chem.* **1980**, *19*, 1980. (b) Bell, S.; Crighton, J. S. *J. Chem. Phys.* **1984**, *80*, 2464.
 6. McIver, J. W.; Komornicki, A. *J. Am. Chem. Soc.* **1972**, *94*, 2625.
 7. Liotard, D. A.; Hawkins, G. D.; Lynch, G. C.; Cramer, C. J.; Truhlar, D. G. *J. Comput. Chem.* **1995**, *16*, 422.
 8. AMSOL 5.0 Program, available from Quantum Chemistry Program Exchange (QCPE) No. 606
 9. (a) Chambers, C. C.; Hawkins, G. D.; Cramer, C. J.; Truhlar, D. G. *J. Phys. Chem.* **1996**, *100*, 16385. (b) Florian, J.; Warshel, A. *J. Phys. Chem. B* **1997**, *101*, 5583.
 10. Ingold, C. K. *Structure and Mechanism in Organic Chemistry*; 2nd ed.; Cornell Univ. Press: Ithaca, 1969; p 457.
 11. (a) Houk, K. N.; Gustabson, S. M.; Black, K. A. *J. Am. Chem. Soc.* **1992**, *114*, 8565. (b) Lee, J. K.; Kim, C. K.; Lee, I. *J. Phys. Chem. A* **1997**, *101*, 2893. (c) Kim, C. K.; Hyun, K. H.; Kim, C. K.; Lee, I. *J. Am. Chem. Soc.* **2000**, *122*, 2294.
 12. Pauling, L. *J. Am. Chem. Soc.* **1947**, *69*, 542.
 13. Hammett, L. P. *Physical Organic Chemistry*; McGrawhill: New York, 1940.
 14. Isaacs, N. *Physical Organic Chemistry*; 2nd ed.; Longman Scientific & Technical; Harlow, 1987; p 380.
 15. Substituent constants, σ^- , are taken from: Ref. (14), Chapter 4.
 16. The pK_a values are taken from: Streitwieser, Jr. A.; Heathcock, C. H. *Introduction to Organic Chemistry*; MacMillan Publishing Company; New York, 1985; p 813.
 17. (a) Rice, F. O.; Teller, E. *J. Chem. Phys.* **1939**, *7*, 199. (b) Hine, J. *Adv. Phys. Org. Chem.* **1977**, *15*, 1.
 18. (a) Lee, I.; Kim, C. K.; Han, I. S.; Lee, H. W.; Kim, W. K.; Kim, Y. B. *J. Phys. Chem. B* **1999**, *103*, 7302. (b) Lee, I.; Kim, C. K.; Lee, I. Y.; Kim, C. K. *J. Phys. Chem. A* **2000**, *104*, 6332.
-